

High spin and shape coexistence in ^{73}Se

M. S. Kaplan,* J. X. Saladin, D. F. Winchell,[†] and H. Takai[‡]

Department of Physics and Astronomy, University of Pittsburgh, Pittsburgh, Pennsylvania 15260

J. Dudek

Centre de Recherches Nucléaires, F-67037 Strasbourg Cedex, France

(Received 28 January 1991)

High-spin states in ^{73}Se were populated via the fusion-evaporation reaction $^{63}\text{Cu}(^{16}\text{O},\alpha p n)^{73}\text{Se}$ at a beam energy of 69 MeV. Several new levels were found in bands of both negative and positive parity. The yrast band of ^{73}Se shows evidence of shape coexistence at low spin. The results of cranked, deformed Woods-Saxon shell-model calculations with self-consistent pairing are compared to the data.

I. INTRODUCTION

Neutron deficient nuclei of mass $A \approx 70-80$ are characterized by shapes and other collective properties which sensitively depend on proton number, neutron number, and angular momentum. This dependence of the collective properties has been associated with the large gaps in the single-particle energy spectra calculated with the use of realistic potentials. Calculations based on the generalized Woods-Saxon potential (see, e.g., Nazarewicz *et al.* [1]) predict competing gaps at different deformations for some nucleon numbers. This is particularly true for the neutron-deficient selenium ($Z=34$) and krypton ($Z=36$) isotopes, where the protons appear to prefer an oblate shape but where neutron numbers of 38–42 favor a strongly deformed ($\beta \approx 0.4$) prolate shape. The shape coexistence phenomena observed [2,3] in $^{72,74}\text{Se}$ and $^{76,78}\text{Kr}$ reflect the competing shape driving tendencies. The study of the high-spin behavior of the neighboring odd nuclei can yield further insight into the nature of the single-particle levels occupied and their effect on the shape of the corresponding even-even core.

The $N=39$ nucleus ^{73}Se is therefore an interesting candidate for study, and here we report the results of a γ - γ coincidence study of the high-spin behavior of this nucleus. Previous work [4,5] established the existence of a collective band built on the $\frac{9}{2}^+$ ground state to spin $I^\pi = \frac{25}{2}^+$ as well as several other positive-parity states. Recent work by Seiffert *et al.* [6], using an $(\alpha, n\gamma)$ reaction, has considerably increased our knowledge of the low-lying states in ^{73}Se . In the present work, we have extended the ground-state band to a tentative $\frac{33}{2}^+$. In addition to the states of positive parity, a rotational band built on a low-lying (25.7 keV) $\frac{3}{2}^-$ state was also established by previous work to $I^\pi = \frac{19}{2}^-$. Here, this band is extended to a tentative level at $\frac{33}{2}^-$. The results are interpreted within the framework of the cranking model and compared to cranked Woods-Saxon-Strutinsky calculations with a fully self-consistent pairing interaction.

II. EXPERIMENTAL PROCEDURE

High-spin states in ^{73}Se were populated utilizing the fusion-evaporation reaction $^{63}\text{Cu}(^{16}\text{O},\alpha p n)^{73}\text{Se}$ at 69 MeV. The ^{16}O beam was obtained with three stage operation of the University of Pittsburgh tandem accelerator. Isotopically enriched (99.9%) ^{63}Cu foils were acquired with two stacked 0.5-mg/cm² self-supporting targets as well as with a 1.0-mg/cm² foil backed with Au. The gamma decay of the residual nucleus was observed with the University of Pittsburgh multidetector array consisting of six high-purity germanium (HPGe) detectors with bismuth germanate (BGO) Compton suppression, and a sum-multiplicity spectrometer (SMS) consisting of 14 independent BGO scintillation detectors. The energies and relative timing of the HPGe and BGO signals were recorded on tape in event-by-event mode. An event trigger was determined by requiring gammas in two or more HPGe detectors and in two or more SMS elements. The latter requirement enhanced the decays from high angular momentum states in the recorded data. Approximately 30×10^6 events were collected with the self-supporting targets and approximately 12×10^6 with the Au backed target. After gain matching (and correcting for Doppler shifts in the self-supporting target data), all possible HPGe coincidence pairs were histogrammed and added to construct 2500×2500 channel coincidence matrices.

III. RESULTS

Figures 1–3 show typical gamma spectra obtained by gating on the strongest transitions in each of the bands observed in ^{73}Se . Energy correlations, intensities, and systematics were used to make tentative spin and parity assignments. In addition, DCO [7] (directional correlations from oriented nuclei) ratios were used to corroborate these assignments where statistics allowed such an analysis. The DCO ratio R_{DCO} is given by

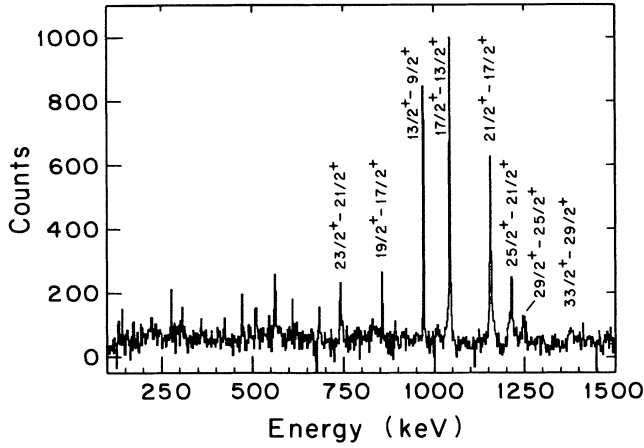


FIG. 1. Gamma spectrum obtained by gating on known negative-parity, positive signature transitions in ^{73}Se .

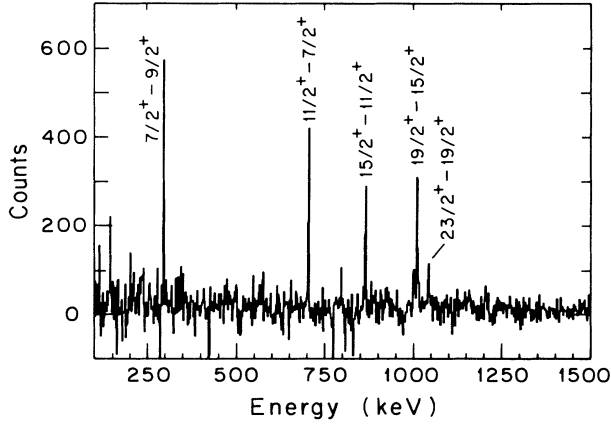


FIG. 2. Gamma spectrum obtained by gating on known positive-parity, negative signature transitions in ^{73}Se .

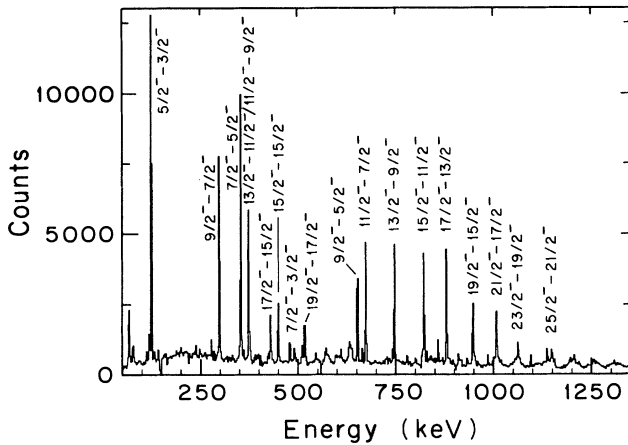


FIG. 3. Gamma spectrum obtained by gating on known negative-parity transitions.

$$R_{\text{DCO}} = \frac{I_{\gamma_1} \text{ at } \theta_1 \text{ gated by } I_{\gamma_2} \text{ at } \theta_2}{I_{\gamma_1} \text{ at } \theta_2 \text{ gated by } I_{\gamma_2} \text{ at } \theta_1},$$

$$\theta_1 = 135^\circ, \theta_2 = 90^\circ. \quad (1)$$

For a gating gamma ray γ_2 of known stretched $E2$ character, the theoretical value of R_{DCO} is unity for a γ_1 of stretched $E2$ character and ranges from nearly 0 to 2 for γ_1 of mixed $E2/M1$ character (unstretched), depending on the multipole mixing ratio. The experimental values of R_{DCO} obtained are shown in Table I. The $E2/M1$ mixing ratio δ can be related to the branching ratio λ according to [8]

$$\lambda \equiv \frac{I_{\gamma}(I \rightarrow I-1)}{I_{\gamma}(I \rightarrow I-2)}$$

$$= \frac{E_{\gamma}^5(I \rightarrow I-2)}{E_{\gamma}^5(I \rightarrow I-1)} \frac{B(E2, I \rightarrow I-1)}{B(E2, I \rightarrow I-2)} \left[1 + \frac{1}{\delta^2} \right]. \quad (2)$$

In the strong-coupling limit, valid for the negative-parity band in ^{73}Se , the $B(E2)$ ratio in Eq. (2) is given by [9]

$$\frac{B(E2, I \rightarrow I-1)}{B(E2, I \rightarrow I-2)} = \frac{2(2I-1)K^2}{(I+1)[(I-1)^2 - K^2]}. \quad (3)$$

Values for δ deduced in this way from the measured branching ratios are given in Table I and are consistent with those from previous work [10,11]. A decay scheme based on the present as well as previous work [4,5,10] is shown in Fig. 4. For some time, there was considerable uncertainty in the spin assignments for the positive-parity ground state and the negative-parity isomeric state. The systematics of the β^+ decay and the decay by electron capture of these states into states in ^{73}As were compatible with the I^{π} assignments of $\frac{7}{2}^+$ and $\frac{1}{2}^-$ or $\frac{9}{2}^+$ and $\frac{3}{2}^-$ for the ground state and the isomeric state [12–14]. Intensity arguments suggested that the isomeric state decays about 27% of the time into the ground state in ^{73}Se , but no γ rays were observed. Konijn *et al.* [15] established in an internal-conversion- γ -coincidence experiment that the isomeric state decays to the ground state via a single $E3$ conversion-electron transition with an energy of 25.7 keV, thus establishing the isomeric state at an excitation energy of 25.7 keV. To our knowledge the only published experiment determining the spin of the ground state has been carried out by Berkes, Hassani, and Massa [16]. That experiment is based on separate determinations of the magnetic moment (by nuclear orientation) and the g factor (by magnetic resonance on oriented nuclei). The result is $I_{g.s.} = \frac{9}{2}$, and thus establishes with fair confidence the spin and parity of the ground state and the isomeric state as $\frac{9}{2}^+$ and $\frac{3}{2}^-$, respectively. A recent redetermination of the g factor by Nishimura, Ohya, and Mutsuro [17] is in excellent agreement with the result of Ref. [16].

In the present study, we observe no transitions connecting states of opposite parity. In the negative-parity band, both $\Delta I=1$ transitions between states of opposite signature and $\Delta I=2$ crossover transitions were observed to high spin. Based on the systematics of gamma intensities in gated spectra, we suggest that the observed $\pi = +1$, $\alpha = -\frac{1}{2}$ states are a rotational sequence and pos-

sibly constitute the signature partner to the ground-state sequence, as shown in Fig. 4. However, the proposed $\pi = +1$, $\alpha = -\frac{1}{2}$ states were populated with too little intensity to perform the DCO analysis, so their spin and

TABLE I. Transitions in ^{73}Se . Assignments based on systematics are denoted by an asterisk.

E_γ (keV)	$I_i^\pi \rightarrow I_f^\pi$	I_γ	$ \delta $	R_{DCO}	$E/M\lambda$
125.1	$\frac{5}{2}^- \rightarrow \frac{3}{2}^-$	100.0(26)		0.60(20)	$E2/M1$
295.4	$\frac{7}{2}^+ \rightarrow \frac{9}{2}^+$	3.9(13)			$E2/M1$
(299)	$(\frac{21}{2}^+ \rightarrow \frac{19}{2}^+)$			0.60(20)	$E2/M1^*$
299.0	$\frac{9}{2}^- \rightarrow \frac{7}{2}^-$	12.5(11)	0.61(24)	0.55(36)	$E2/M1$
354.1	$\frac{7}{2}^- \rightarrow \frac{5}{2}^-$	27.7(21)	0.18(3)	0.49(13)	$E2/M1$
373	$\frac{13}{2}^- \rightarrow \frac{11}{2}^-$	12.4(48)	1.04(6)	0.32(12)	$E2/M1$
375	$\frac{11}{2}^- \rightarrow \frac{9}{2}^-$				
430.6	$\frac{17}{2}^- \rightarrow \frac{15}{2}^-$	4.5(5)	0.17(24)	0.33(23)	$E2/M1$
449.9	$\frac{15}{2}^- \rightarrow \frac{13}{2}^-$	7.5(6)	0.19(5)	0.87(42)	$E2/M1^*$
(472)	$(\frac{25}{2}^+ \rightarrow \frac{23}{2}^+)$				$E2/M1^*$
490.4	$\frac{21}{2}^- \rightarrow \frac{19}{2}^-$	2.7(3)	0.11(6)		$E2/M1^*$
517.3	$\frac{19}{2}^- \rightarrow \frac{17}{2}^-$	9.1(5)	0.15(4)		$E2/M1^*$
572.7	$\frac{23}{2}^- \rightarrow \frac{21}{2}^-$	4.1(3)	0.07(3)		$E2/M1^*$
578.0	$\frac{25}{2}^- \rightarrow \frac{23}{2}^-$	2.6(14)	0.055(55)		$E2/M1$
653.8	$\frac{9}{2}^- \rightarrow \frac{5}{2}^-$	31.9(12)		1.00(26)	$E2$
674.3	$\frac{11}{2}^- \rightarrow \frac{7}{2}^-$	28.8(31)		0.96(41)	$E2$
703.9	$\frac{11}{2}^- \rightarrow \frac{7}{2}^-$	8.7(25)			$E2^*$
742.5	$\frac{23}{2}^+ \rightarrow \frac{21}{2}^+$	14.4(10)			$E2/M1^*$
747.9	$\frac{13}{2}^- \rightarrow \frac{9}{2}^-$	31.1(26)		0.74(40)	$E2$
823.0	$\frac{15}{2}^- \rightarrow \frac{11}{2}^-$	28.7(22)			$E2^*$
856.9	$\frac{19}{2}^+ \rightarrow \frac{17}{2}^+$	5.7(9)	0.08(5)		$E2/M1^*$
864	$\frac{15}{2}^+ \rightarrow \frac{11}{2}^+$	13.9(25)			$E2$
880.6	$\frac{17}{2}^- \rightarrow \frac{13}{2}^-$	31.4(25)		0.68(21)	$E2$
891.8	$\frac{15}{2}^+ \rightarrow \frac{13}{2}^+$	7.4(14)	0.15(11)		$E2/M1$
947.9	$\frac{19}{2}^- \rightarrow \frac{15}{2}^-$	19.9(17)		1.20(52)	$E2$
971.6	$\frac{13}{2}^+ \rightarrow \frac{9}{2}^+$	42.1(33)			$E2^*$
999.4	$\frac{11}{2}^+ \rightarrow \frac{9}{2}^+$	10.1(10)	0.43(31)		$E2/M1$
1008.0	$\frac{21}{2}^- \rightarrow \frac{17}{2}^-$	12.0(12)			$E2^*$
1009.0	$\frac{19}{2}^+ \rightarrow \frac{15}{2}^+$				$E2^*$
1041.7	$\frac{23}{2}^+ \rightarrow \frac{19}{2}^+$				$E2^*$
1043.8	$\frac{17}{2}^+ \rightarrow \frac{13}{2}^+$	47.2(38)		1.00(25)	$E2$
1063.0	$\frac{23}{2}^- \rightarrow \frac{19}{2}^-$	6.4(10)			$E2^*$
1148.9	$\frac{25}{2}^- \rightarrow \frac{21}{2}^-$	5.1(9)			$E2^*$
1156.9	$\frac{21}{2}^+ \rightarrow \frac{17}{2}^+$	29.6(26)		0.59(20)	$E2^*$
1206	$\frac{27}{2}^- \rightarrow \frac{23}{2}^-$				$E2^*$
1214.4	$\frac{25}{2}^+ \rightarrow \frac{21}{2}^+$	16.2(27)			$E2^*$
1249.9	$\frac{29}{2}^+ \rightarrow \frac{25}{2}^+$	11.9(20)			$E2^*$
1265	$\frac{29}{2}^- \rightarrow \frac{25}{2}^-$				$E2^*$
1307	$\frac{31}{2}^- \rightarrow \frac{27}{2}^-$				$E2^*$
1378.1	$\frac{33}{2}^+ \rightarrow \frac{29}{2}^+$	9.6(21)			$E2^*$
1381	$\frac{33}{2}^- \rightarrow \frac{29}{2}^-$				$E2^*$

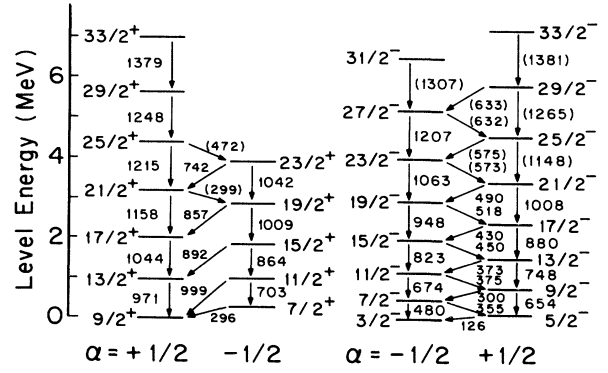


FIG. 4. Decay scheme for ^{73}Se based on the present and previous work. The $\frac{3}{2}^-$ isomeric state is at an excitation energy of 25.7 keV (see text).

parity assignments remain tentative.

Experimental total Routhians are plotted in Fig. 5. The negative-parity band exhibits negligible signature splitting up to the highest spins observed, typical for the strongly coupled negative-parity rotational bands observed in neighboring isotones [4,10,18,19,20]. By contrast, the positive-parity states display large signature splitting, with the $\frac{7}{2}^+$ state lying above the $\frac{9}{2}^+$ ground state.

Plots of I_x and $\mathcal{J}^{(1)}$ vs $\hbar\omega$ for each set of parity and signature quantum numbers are shown in Figs. 6 and 7. In the ground-state band, $\mathcal{J}^{(1)}$ rises rapidly with increasing $\hbar\omega$ until $I = \frac{29}{2}$, where it begins to flatten. This suggests a possible transition from vibration-like behavior to rotationlike behavior near spin $\frac{29}{2}$. The 971 keV ($\frac{13}{2}^+ \rightarrow \frac{9}{2}^+$) transition is of higher energy than any $2^+ \rightarrow 0^+$ or analogous $\Delta I=2$ transition to the ground state known in this region, again suggesting a vibrational structure. The plots for the negative-parity sequences, on the other hand, indicate good rotational behavior.

IV. DISCUSSION

A. General features

Experimentally, the effects of shape coexistence have been well established [21,22] in the neighboring $^{72,74}\text{Se}$

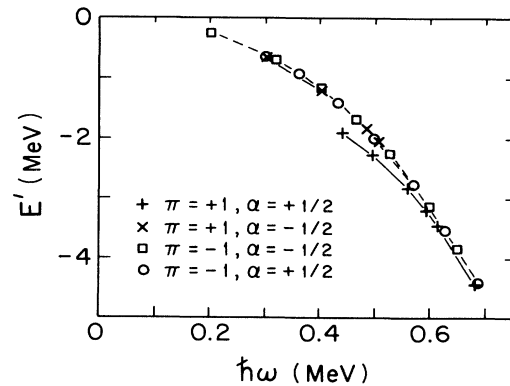


FIG. 5. Experimentally determined total Routhians for the decay sequences observed in ^{73}Se .

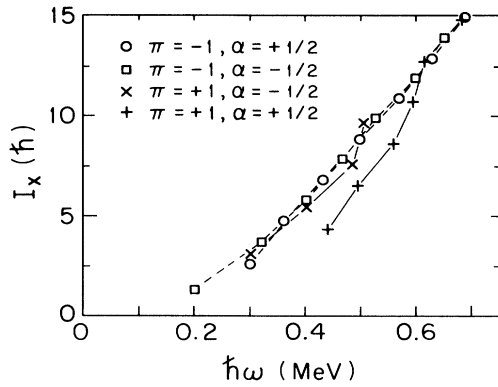


FIG. 6. Angular momentum I_x as a function of $\hbar\omega$.

even-even nuclei. Until recently it was thought that the coexistence occurred between a vibrational band built on a nearly spherical oblate state and a well-deformed prolate rotational band. A recent study by Cottle *et al.* [23] suggests that, in ^{74}Se , the coexisting bands are both built on well-deformed states. The effect of an odd nucleon added to a shape-coexistent even-even core is not well understood. In some cases, such as in ^{73}Br , the odd nucleon has been found to polarize the core, thus stabilizing one of the shapes [24–27] and quenching the coexistence.

A Nilsson diagram calculated using a deformed Woods-Saxon potential is shown in Fig. 8. For $N=39$, the lowest positive-parity neutron orbital is predicted to have $\Omega = \frac{3}{2}$ or $\frac{5}{2}$ for axially symmetric prolate shapes, and $\Omega = \frac{9}{2}$ for axially symmetric oblate shapes, although strong mixing among the $g_{9/2}$ Nilsson orbitals is expected for near-spherical or triaxial shapes. The ground-state spin value of $\frac{9}{2}$ might therefore suggest that the nucleus is oblate and that the ground-state band is built on the Nilsson $[404]_{\frac{9}{2}}$ orbital. Another possibility is that the ground-state band is a decoupled band built on the even-even core. The results of a least-squares fit of the positive-parity level energies to the rotational model expression for a decoupled band [9]

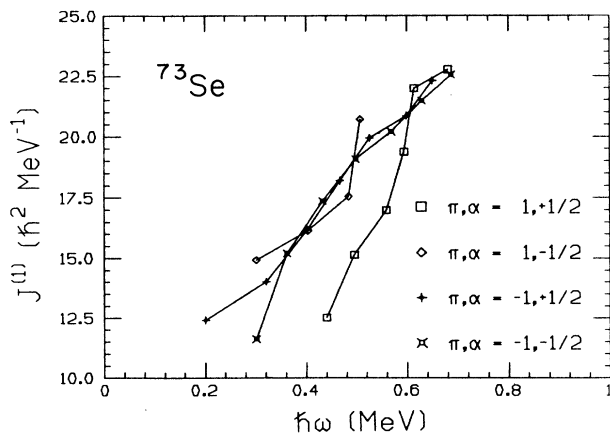


FIG. 7. Kinematic moment of inertia $J^{(1)}$ as a function of $\hbar\omega$.

$$E = AI(I+1) + A_1(-1)^{I+1/2}(I+\frac{1}{2}) \quad (4)$$

is shown in Fig. 9. The parameters giving the best fit are $A=26.1$ keV, $A_1=18.8$ keV, which gives a decoupling parameter $a = A_1/A=0.72$, slightly smaller than the value expected for a pure decoupled band built on a $K^\pi=0^+$ core. The discrepancy between the fit and the experimental data for the lower members of the band might be an indication of shape coexistence between rotational and vibrational structures. In Fig. 10 the $\frac{9}{2}^+$ band in ^{73}Se is compared to the ground-state bands of ^{72}Se and ^{74}Se . It can be seen that the level spacings between the $\alpha = +\frac{1}{2}$ states in ^{73}Se are comparable to the spacings found in the even-even nuclei. This again suggests that the ground-state band in ^{73}Se is decoupled.

While strong evidence [28] exists for $\Omega = \frac{9}{2}$ collective oblate bands in $^{69,71}\text{Se}$, the large signature splitting displayed by the positive-parity states in ^{73}Se does not support such an interpretation in this nucleus. Collective bands built on high Ω orbitals in well-deformed, axially symmetric nuclei should be subject to little mixing with the $\Omega = \frac{1}{2}$ orbital responsible for signature splitting. Because of the triaxial and/or vibrational nature of the positive-parity band in ^{73}Se , an intermediate value of $K = \frac{5}{2}$ was chosen to construct the plots shown in Figs. 5–7.

It is interesting to note that in contrast to the situation in ^{73}Se , the ground state of the neighboring isotope ^{75}Kr

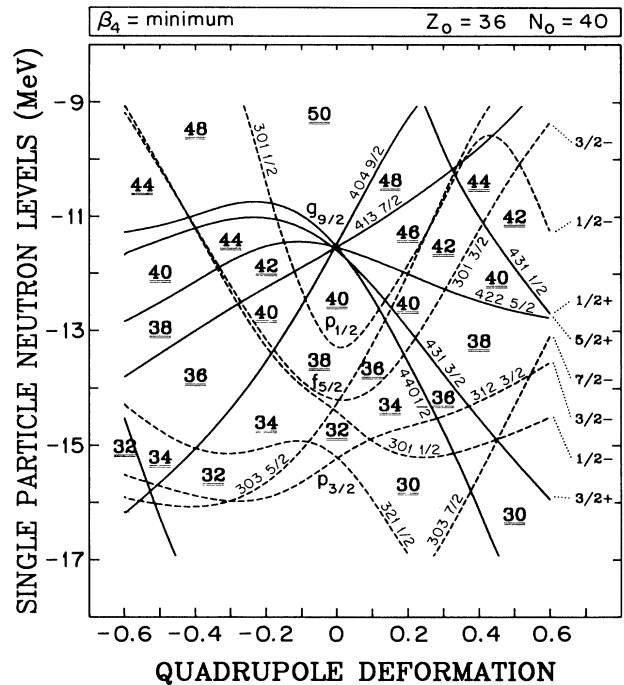


FIG. 8. Nilsson diagram for neutrons calculated with a deformed Woods-Saxon potential. Positive-parity orbitals are indicated by solid lines, negative-parity by dashed lines. Underlined numbers in the gaps indicate the number of nucleons needed to fill the orbitals.

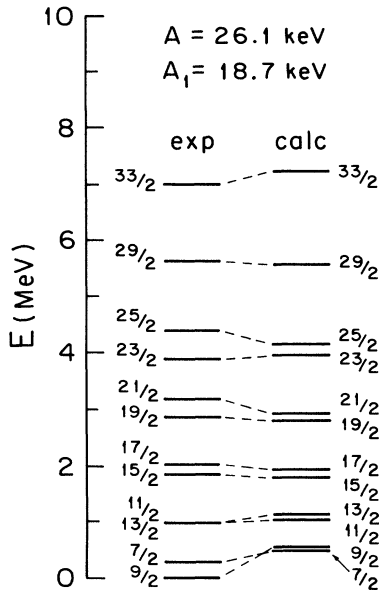


FIG. 9. Comparison of experimental levels to the results of a least-squares fit of Eq. (2). The coefficients from the fit are listed at the top of the figure.

is $\frac{5}{2}^-$ and the rotational sequence built on it has been interpreted [18–20] successfully in terms of a Nilsson $[422]_{\frac{5}{2}}^-$ quasiparticle strongly coupled to a deformed ($\beta \approx 0.4$) core. Therefore, it appears that the addition of two protons to ^{73}Se has a dramatic effect on the shape. It can be seen in the Nilsson diagram (Fig. 8) that for $Z=34$, the nucleus will in general prefer less deformed shapes than for $Z=36$, making the $[422]_{\frac{5}{2}}^-$ orbital un-

available to the odd neutron.

Rotational bands of negative parity with a structure similar to that observed in ^{73}Se are common to many nuclei [4,10,19,20] of this region. These bands have generally been interpreted as collective rotations built on a pure Nilsson configuration of $[301]_{\frac{3}{2}}^-$. Doppler-shift-attenuation lifetime measurements [5,8] in ^{73}Se , which show strong collective transition between the states in the $\frac{5}{2}^-$ sequence and those of the $\frac{3}{2}^-$ sequence [with $B(E2) \approx 60-70$ single-particle units], support this interpretation. The strong cascade ($\Delta I=1$) transitions we observe to high spins lend further support. It should be noted, however, that in ^{75}Se the $\frac{3}{2}^-$ and $\frac{5}{2}^-$ states were assigned different Nilsson configurations [29] ($[303]_{\frac{5}{2}}^-$ for the latter) on the basis of spectroscopic factors from transfer reactions.

B. Interpretation

In order to better understand the nature of the single-particle orbitals and the shape of ^{73}Se , model calculations using a cranked Woods-Saxon potential and Strutinsky shell correction were performed. As a first step, total energy surfaces, calculated without any pairing correlation, were produced for several spin values. (See Winchell *et al.* [20] and references quoted therein for a description of these calculations). The minimum energy on these surfaces was found at deformation parameters $\beta_2=0.380$, $\gamma=-2^\circ$ for the positive-parity band. Using these shape parameters, calculations were carried out including monopole pairing. The version of the code used treats pairing at all values of ω self-consistently until the pairing gap drops to a preset value, at which point the pairing gap is kept constant. In Fig. 11 the experimentally determined ground band moment of inertia is compared to the

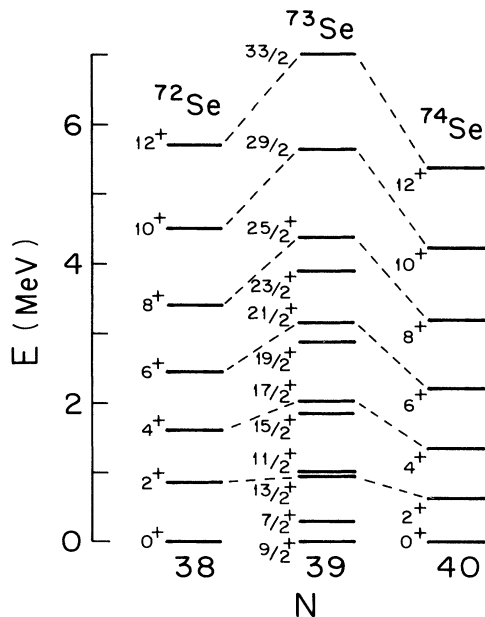


FIG. 10. Comparison of the ground-state bands of ^{72}Se , ^{73}Se , and ^{74}Se .

^{73}Se Moments of inertia

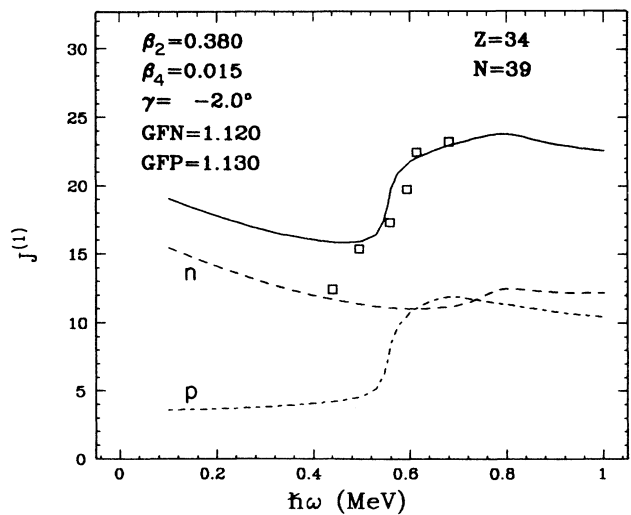


FIG. 11. Experimental versus calculated moments of inertia. Squares indicate the experimental points and the solid line shows the result of the calculations. The dashed and dot-dashed lines show, respectively, the neutron and proton contributions to the calculated value.

moment of inertia given by the calculations. This comparison is used to adjust the pairing strength parameters G_{neut} and G_{prot} for further calculations. With the exception of the lowest point, corresponding to the $\frac{13}{2}^+$ to $\frac{9}{2}^+$ transition, it was possible to obtain a good fit to the data.

Quasiparticle Routhians calculated with the same deformation parameters are shown in Fig. 12. The signature splitting between the lowest two neutron Routhians, which have positive parity, is considerably less than that seen experimentally in the ground-state band. In addition, the experimentally observed signature inversion is not seen here. The lowest negative-parity neutron Routhians in Fig. 12 are in somewhat better agreement with the experimental negative-parity Routhians, where little or no signature splitting is observed.

Total Routhian surfaces (TRS's) for ^{73}Se were produced by performing self-consistent pairing calculations for 255 points on the (β_2, γ) plane at several values of angular frequency ω . The Routhians were minimized at each point with respect to the deformation parameter β_4 . Surfaces corresponding to four values of ω are shown in Fig. 13. In calculating these surfaces, it was required that the odd neutron occupy the lowest $\pi = +1, \alpha = +\frac{1}{2}$ quasiparticle state. The surface corresponding to $\hbar\omega = 0.0$ MeV shows a great deal of gamma softness, with shallow minima occurring on both the oblate and prolate axes. At $\hbar\omega = 0.4$ MeV, the surface is still quite gamma

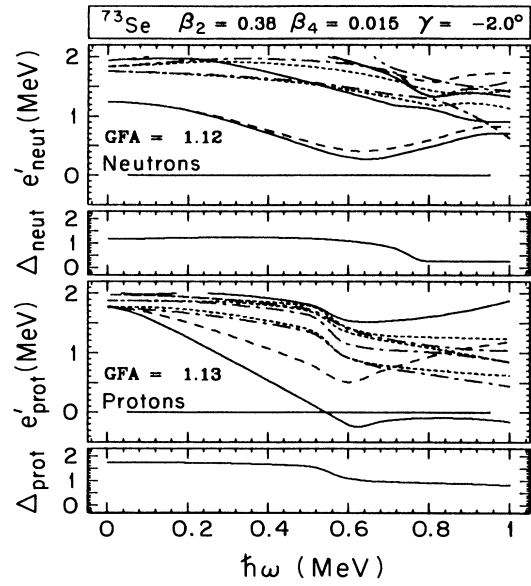


FIG. 12. Calculated quasiparticle Routhians for neutrons and protons in ^{73}Se . Routhians are labeled by parity and signature quantum numbers: solid line ($\pi = +1, \alpha = +\frac{1}{2}$), long-dashed line ($+1, -\frac{1}{2}$), short-dashed line ($-1, +\frac{1}{2}$), and dot-dashed line ($-1, -\frac{1}{2}$). Plots of the calculated, Δ , are shown below the Routhian plots.

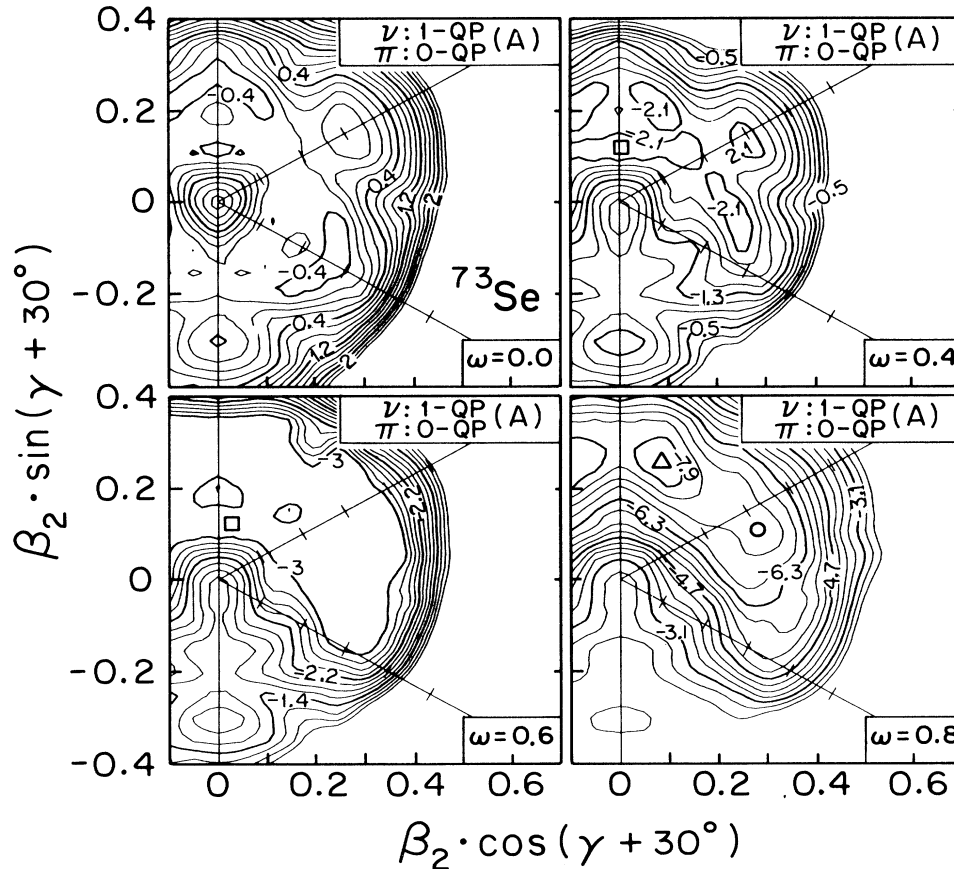


FIG. 13. Total Routhian surfaces corresponding to the positive-parity decay sequence in ^{73}Se . Surfaces were calculated requiring a $(\pi, \alpha) = (+1, +\frac{1}{2})$ configuration. The contour interval is 0.2 MeV.

soft, but there exist a number of fairly well-defined minima all within about 100 keV of each other. The situation here is somewhat different than seen in the calculations of Cottle *et al.* [23] for ^{74}Se , in that a nearly spherical, oblate minimum is predicted for ^{73}Se . This minimum is indicated by an open square in the figure. The main difference between the calculations of Ref. [23] and our own calculations is in the treatment of pairing. Reference [23] treats pairing self-consistently only at $\omega=0$, while we treat it self-consistently at all values of ω . Our procedure leads to an increase in the pairing strength of 12% and 13% for neutrons and protons, respectively. Using our procedure to calculate total Routhian surfaces in ^{74}Se , we obtain qualitative agreement with the results of Ref. [23] with regard to the positions of the minima. Thus the differences between the surfaces for ^{73}Se and ^{74}Se result from the addition of a single neutron and not from differences in the calculations. At higher frequencies the degree of gamma softness lessens, until, at $\hbar\omega=0.8$ MeV, there are just two minima left. These occur near the prolate axis (open circle) and at a deformation corresponding to a less collective triaxial shape (open triangle).

On the basis of the calculations, it seems likely that

shape coexistence plays an important role in the structure of ^{73}Se at low spins. In particular, the existence of a near-spherical, oblate minimum at low angular frequencies might indicate a mixing between bands based on vibrational and rotational excitations, as has been suggested for ^{72}Se and for $^{74,76}\text{Kr}$.

TRS's calculated for negative-parity states are shown in Fig. 14. These are similar to the surfaces shown in Fig. 13 in that the gamma softness occurring at low angular frequency gradually lessens at higher values of $\hbar\omega$. One important difference is that the oblate minimum found on the positive-parity surface at $\hbar\omega=0.4$ MeV does not occur for the negative-parity case (the contour near $\beta_2=0.2$, $\gamma=60^\circ$ indicates a local *maximum*). Therefore the surfaces agree with the experimental observation that the negative-parity band has a more rotational character than the positive-parity band.

V. SUMMARY AND CONCLUSIONS

Several new states were added to the high-spin spectrum of ^{73}Se , including a proposed $(\pi, \alpha) = (+1, -\frac{1}{2})$ rotational sequence. Fits to both a decoupled rotor formula and cranked shell-model calculations with pairing indi-

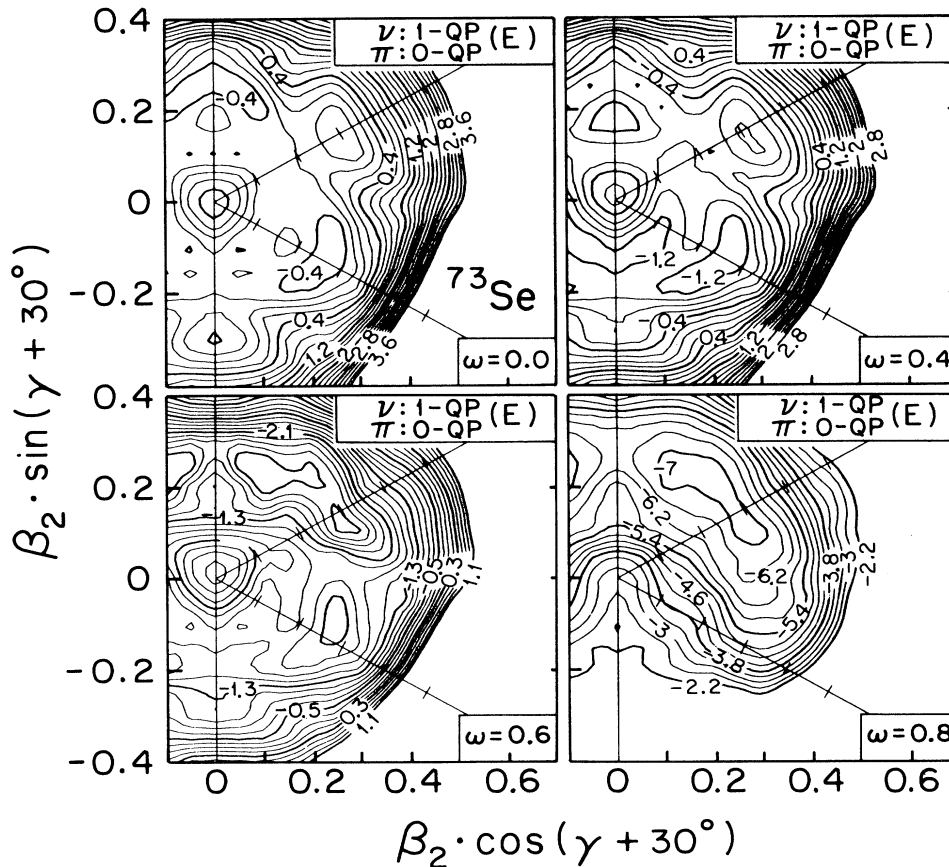


FIG. 14. Total Routhian surfaces corresponding to the positive-parity decay sequence in ^{73}Se . Surfaces were calculated requiring a $(\pi, \alpha) = (-1, +\frac{1}{2})$ configuration. The contour interval is 0.2 MeV.

cate that the character ground-state band is not that of a good rotor at low spins. Calculated total Routhian surfaces indicate a great deal of gamma softness and a number of competing minima for this nucleus, especially for the ground-state band. This is remarkably different from the $N=39$ nucleus ^{75}Kr , for which the ground-state band was well described by the cranking model. In addition, it is dissimilar to the nucleus ^{73}Br , in which the odd proton, added to the even-even ^{72}Se core, removes the shape coexistence effect. In general, the negative-parity band in ^{73}Se is well explained in terms of an odd particle coupled to a deformed rotating core.

ACKNOWLEDGMENTS

We wish to thank Professor C. M. Vincent and Professor R. A. Sorenson for many illuminating discussions. We acknowledge helpful comments from Professor S. Tabor (FSU) and Dr. L. Funke from the Zentral Institut für Kernforschung, Rosendorf, Germany. We also thank M. Metlay and L. Wehner for help with data acquisition and analysis. This work was funded by the National Science Foundation. All calculations were performed at the University of Pittsburgh Supercomputer Center.

-
- *Present address: Nuclear Physics Laboratory, University of Washington, Seattle, WA 98195.
 †Present address: Oak Ridge National Laboratory, Oak Ridge, TN 37830.
 ‡Present address: Department of Physics, Brookhaven National Laboratory, Upton, NY 11973.
- [1] W. Nazarewicz, J. Dudek, R. Bengtsson, T. Bengtsson, and I. Ragnarsson, *Nucl. Phys.* **A435**, 397 (1985).
 [2] J. H. Hamilton, H. C. Crowell, R. L. Robinson, A. V. Ramayya, W. E. Collins, R. M. Ronningen, V. Maruhn-Rezwani, J. A. Maruhn, N. C. Singhal, H. J. Kim, R. O. Sayer, T. Magee, and L. C. Whitlock, *Phys. Rev. Lett.* **36**, 340 (1976).
 [3] R. B. Piercey, A. V. Ramayya, J. H. Hamilton, J. X. Sun, Z. Z. Zhao, R. L. Robinson, and H. J. Kim, *Phys. Rev. C* **25**, 1941 (1982).
 [4] K. O. Zell, B. Heits, W. Gast, D. Hippe, W. Schuh, and P. von Brentano, *Z. Phys. A* **279**, 373 (1976).
 [5] Li Guangsheng, L. Cleeman, J. Eberth, T. Heck, W. Neumann, M. Nolte, and J. Roth, *Chin. J. Phys.* **5**, 217 (1985).
 [6] F. Seiffert, A. Grandérath, A. Dewald, W. Lieberz, U. Neumeyer, E. Ott, J. Theuerkauf, R. Wirowski, H. Wolters, K. O. Zell, P. von Brentano, K. Schiffer, D. Alber, and K. H. Maier, *Z. Phys. A* **336**, 241 (1990).
 [7] K. S. Krane, R. M. Steffen, and R. M. Wheeler, *Nucl. Data Tables* **11**, 351 (1953).
 [8] H. Morinaga and T. Yamazaki, *In Beam Gamma-ray Spectroscopy* (North-Holland, Amsterdam, 1976).
 [9] A. Bohr and B. R. Mottelson, *Nuclear Structure* (Benjamin Inc., New York, 1975), Vol. II.
 [10] A. Dewald, A. Gelerg, U. Kaup, R. Richter, K. O. Zell, and P. von Brentano, *Z. Phys. A* **326**, 508 (1987).
 [11] F. Seiffert *et al.*, *^{73}Se Investigated by the $(\alpha, n\gamma)$ Reaction, in Nuclear Structure of the Zirconium Region* (Springer-Verlag, Berlin, 1988).
 [12] G. Murray, W. J. K. White, J. C. Willmott, and R. F. Entwistle, *Phys. Lett.* **28B**, 35 (1968).
 [13] K. W. Marlow and A. Faas, *Nucl. Phys.* **A132**, 339 (1969).
 [14] B. O. Ten Brink, P. Yan Nes, C. Hoetmar, and H. Verheul, *Nucl. Phys.* **A338**, 24 (1980).
 [15] J. Konijn, B. Klank, D. L. Spenny, and R. A. Ristinen, *Nucl. Phys.* **A138**, 577 (1969).
 [16] I. Berkes, R. Hassani, and M. Massaq, *Phys. Rev. C* **38**, 2329 (1988).
 [17] K. Nishimura, S. Ohya, and N. Mutsuro, *J. Phys. Soc. Jpn.* **56**, 3512 (1987).
 [18] G. Garcia Bermudez, C. Baktash, and C. J. Lister, *Phys. Rev. C* **30**, 43 (1987).
 [19] M. A. Herath-Banda, A. V. Ramayya, L. Cleeman, J. Eberth, J. Roth, T. Heck, N. Schmal, T. Mylaeus, W. Koenig, B. Martin, K. Bethge, and G. A. Leander, *J. Phys. G* **13**, 43 (1987).
 [20] D. F. Winchell, M. S. Kaplan, J. X. Saladin, H. Takai, J. J. Kolata, and J. Dudek, *Phys. Rev. C* **40**, 2672 (1989).
 [21] B. Wörmann, K. P. Lieb, R. Diller, L. Lühmann, J. Keinonen, L. Cleemann, and J. Eberth, *Nucl. Phys.* **A431**, 170 (1984).
 [22] J. H. Hamilton, A. V. Ramayya, W. T. Pinkston, R. M. Ronningen, G. Garcia-Bermudez, H. K. Carter, R. L. Robinson, H. J. Kim, and R. O. Sayer, *Phys. Rev. Lett.* **32**, 239 (1974).
 [23] P. D. Cottle, J. W. Holocomb, T. D. Johnson, K. A. Stuckey, S. L. Tabor, and P. C. Womble, *Phys. Rev. C* **42**, 1254 (1990).
 [24] J. Heese, K. P. Lieb, L. Lühmann, S. Ulbig, B. Wörmann, D. Alber, H. Grawe, H. Haas, and B. Spellmeyer, *Phys. Rev. C* **36**, 2409 (1987).
 [25] B. Wörmann, J. Heese, K. P. Lieb, L. Lühmann, F. Raether, D. Alber, H. Grawe, and B. Spellmeyer, *Z. Phys. A* **322**, 171 (1985).
 [26] L. Lühmann, M. Debray, K. P. Lieb, W. Nazarewicz, B. Wörmann, J. Eberth, and T. Heck, *Phys. Rev. C* **31**, 828 (1985).
 [27] L. Lühmann, K. P. Kieb, C. J. Lister, B. J. Varleg, J. W. Olness, and H. G. Price, *Europhys. Lett.* **1**, 623 (1986).
 [28] M. Wiosna, J. Busch, J. Eberth, M. Liebchen, T. Mylaeus, N. Schmal, R. Sefzig, S. Skoda, and W. Teichert, *Phys. Lett. B* **200**, 255 (1988).
 [29] K. O. Zell, H.-G. Friedrichs, B. Heits, D. Hippe, H. W. Schuh, P. von Brentano, and C. Protop, *Z. Phys. A* **276**, 371 (1976).